www.nature.com/lsa

### **ORIGINAL ARTICLE**

# Transforming the cost of solar-to-electrical energy conversion: Integrating thin-film GaAs solar cells with non-tracking mini-concentrators

Kyusang Lee<sup>1</sup>, Jaesang Lee<sup>1</sup>, Bryan A Mazor<sup>2</sup> and Stephen R Forrest<sup>1,2,3</sup>

Practical solar energy solutions must not only reduce the cost of the module, but also address the substantial balance of system costs. Here, we demonstrate a counter-intuitive approach based on gallium arsenide solar cells that can achieve extremely low-cost solar energy conversion with an estimated cost of only 3% that of conventional gallium arsenide solar cells using an accelerated, non-destructive epitaxial lift-off wafer recycling process along with a lightweight, thermoformed plastic, truncated mini-compound parabolic concentrator that avoids the need for active solar tracking. Using solar cell/concentrator assemblies whose orientations are adjusted only a few times per year, the annual energy harvesting is increased by 2.8 times compared with planar solar cells without solar tracking. These results represent a potentially drastic cost reduction in both the module and the balance of system costs compared with heavy, rigid conventional modules and trackers that are subject to wind loading damage and high installation costs.

Light: Science & Applications (2015) 4, e288; doi:10.1038/lsa.2015.61; published online 8 May 2015

Keywords: concentrator; cost per Watt; epitaxial lift-off; plastic substrate; thin-film GaAs solar cell

#### INTRODUCTION

Due to the nearly unlimited abundance of solar energy, photovoltaic cells that convert sunlight directly into electricity represent the most promising alternative energy source. However, cost-efficient solar-toelectrical energy harvesting remains a major hurdle that must be fully surmounted if we are to expect its eventual widespread deployment. Considerable efforts in developing photovoltaics have therefore focused on achieving low cost while increasing their power conversion efficiency (PCE).<sup>1-4</sup> One recent achievement has been the demonstration of thin-film GaAs solar cells approaching their thermodynamic efficiency limit.<sup>5–8</sup> However, the cost reduction long promised by the epitaxial lift-off (ELO) process has primarily been limited by the inability to fully recover the original wafer surface quality after each growth, leading to a limited number of times that the substrate can be recycled due to the accumulation of defects and to wafer thinning incurred by chemo-mechanical polishing.<sup>9-13</sup> Furthermore, high PCE alone does not necessarily translate into low-cost solar energy production when expensive active materials and fabrication processes are used in their manufacture. As an alternative to simply improving PCE, solar concentrators have been demonstrated as a means for reducing the use of costly active solar cell materials.<sup>14,15</sup> However, most concentrators suffer from a significant roll-off in efficiency at large light incident angles and can also result in high cell operating temperatures, thereby necessitating expensive active solar tracking and solar cell cooling systems.16

Here, we demonstrate that thin-film GaAs solar cells produced by an accelerated non-destructive ELO (ND-ELO) fabrication process that are integrated with simple thermoformed mini-concentrators can lead to a dramatic reduction in the cost of the production of electricity via solar energy harvesting. This approach reduces cell material and fabrication costs to only 3% that of analogous substrate-based GaAs cells, and only 11% that of ELO-processed GaAs solar cells, while the optical system maximizes the annual energy output using highly truncated two-dimensional mini-compound parabolic concentrators (CPCs). This low-profile concentrator provides a very thin and lightweight module with improved off-angle sunlight absorption compared to conventional concentrators both in direct and in diffuse sunlight with only minor losses. Our approach, therefore, eliminates the need for high concentration factor optics that require expensive and heavy solar tracking paraphernalia. Furthermore, the unique geometry of thin-film GaAs solar cells mounted on a heat-sinking metal layer enables operation at or near room temperature without active cooling, even for concentration factors approaching 4×, representing a reduction of over 40 °C compared to substrate-based GaAs solar cells.

#### MATERIALS AND METHODS Epitaxial growth

The solar cell epitaxial layer structures are grown by gas-source molecular beam epitaxy (GSMBE) on Zn-doped (100) p-GaAs substrates. The

<sup>&</sup>lt;sup>1</sup>Department of Electrical Engineering and Computer Science, University of Michigan, Ann Arbor, MI 48109, USA; <sup>2</sup>Department of Physics, University of Michigan, Ann Arbor, MI 48109, USA and <sup>3</sup>Department of Material Science and Engineering, University of Michigan, Ann Arbor, MI 48109, USA

Correspondence: S Forrest, Department of Electrical Engineering and Computer Science, University of Michigan, Ann Arbor, MI 48109, USA E-mail: stevefor@umich.edu

Received 8 November 2014; revised 2 February 2015; accepted 4 February 2015; accepted article preview online 5 February 2015

Integrated GaAs cells with parabolic concentrators K Lee *et al* 

growth starts with a GaAs buffer layer (0.2 µm thick) followed by InGaP/GaAs (100 nm/100 nm) protection layers and an AlAs (20 nm) sacrificial layer. Next, an inverted active device region is grown as follows:  $5 \times 10^{18}$  cm<sup>-3</sup> Be-doped GaAs (0.15 µm) contact layer,  $2 \times 10^{18}$  cm<sup>-3</sup> Be-doped Al<sub>0.20</sub>In<sub>0.49</sub>Ga<sub>0.31</sub>P (0.025 µm) window,  $1 \times 10^{18}$  cm<sup>-3</sup> Be-doped p-GaAs (0.15 µm) emitter layer,  $2 \times 10^{17}$  cm<sup>-3</sup> Si-doped n-GaAs (3.0 µm) base layer,  $6 \times 10^{17}$  cm<sup>-3</sup> Si-doped n-GaAs (0.1 µm) contact layer and  $5 \times 10^{18}$  cm<sup>-3</sup> Si-doped n-GaAs (0.1 µm) contact layer. The GaAs/ AlAs layers are grown at 600 °C, and the Al<sub>0.20</sub>In<sub>0.49</sub>Ga<sub>0.31</sub>P/In<sub>0.49</sub>Ga<sub>0.51</sub>P layers are grown at 480 °C.

#### Pre-mesa patterning, cold weld bonding and epitaxial lift-off

Figure 1a shows the schematic illustration of the process flow for pre-mesa patterning, cold welding and ND-ELO. Mesas of 2.5 mm×6.5 mm Cr/Au (4 nm/350 nm) are patterned by photolithography using a LOR 3A and S-1827 (Microchem, Newtown, MA, USA) bi-layer photoresist as a mask and H<sub>3</sub>PO<sub>4</sub>:H<sub>2</sub>O<sub>2</sub>:deionized H<sub>2</sub>O (3:1:25) and HCl:H<sub>3</sub>PO<sub>4</sub> (3:1) as etchants for GaAs and InGaP, respectively. The patterned Au on the epitaxial GaAs wafer is bonded to the Au-coated 25 µm thick Kapton<sup>®</sup> sheet using an EVG 520 wafer bonder at ~10<sup>-5</sup> torr. Then, a pressure of 4 MPa with an 80 N s<sup>-1</sup> ramp rate is applied to the 2-inch-diameter substrate to establish a bond between the Au films. The temperature is increased to 230 °C at 25 °C min<sup>-1</sup> and held at that temperature for 8 min. The substrate is then rapidly cooled. To apply uniform pressure, a soft graphite sheet is inserted between the sample and the press head. Once the GaAs substrate fully adheres to the Kapton<sup>®</sup> sheet, the thin active device region is removed from its parent substrate using ND-ELO.<sup>9</sup> The sample is immersed in a 20% HF:H<sub>2</sub>O solution maintained at 60 °C while

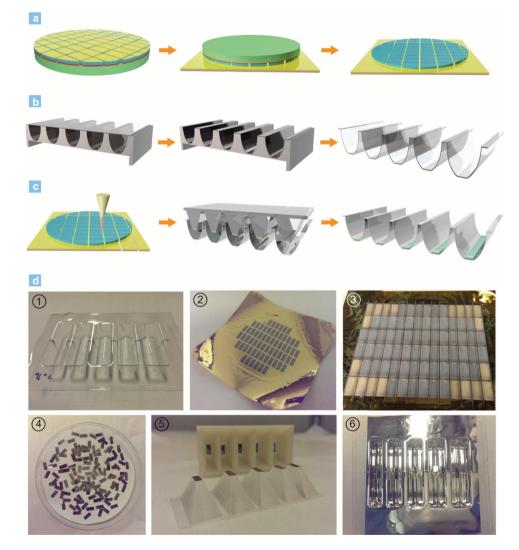


Figure 1 Illustration and photographs of the fabrication steps for integration of CPCs with thin-film GaAs solar cells. (a) Proceeding left to right: Mesas are prepatterned prior to the ND-ELO by selective etching that stops at the AIAs sacrificial layer (red). The sample is then bonded onto the Au-coated Kapton® sheet *via* coldwelding. The third step shows the sample following ND-ELO. (b) The PETG sheet is fixed on top of the metal mold and is then thermoformed into its final shape by applying heat and vacuum. Finally, the mini-CPCs are detached from the mold. (c) The solar cell-Kapton® sheet assembly is separated into individual bars using laser dicing. Then, each bar is transfer printed onto the mini-CPCs using a PDMS stamp *via* low-pressure cold-welding. The last schematic shows the integrated thin-film solar cells and mini-CPC after a reflective metal coating is deposited onto the CPC array surface. (d) Photographs of ① PETG sheet after thermoforming into CPCs, ② fabricated thin-film GaAs solar cells on a Kapton® sheet after mesa pre-patterning and ND-ELO, ③ thin-film GaAs solar cells following dicing, ④ separated and cleaned solar cell bars, ⑤ PDMS stamps and 3D printed mold used in transfer printing and ⑥ integrated thin-film GaAs solar cells integrated with plastic mini-CPCs. CPC, compound parabolic concentrator; ND-ELO, non-destructive epitaxial lift-off.

#### Solar cell fabrication

Following lift-off, the thin-film active region and flexible plastic host are fixed to a rigid substrate using Kapton® tape. The front surface contact grid is photolithographically patterned using the LOR 3A and S-1827 (Microchem) bi-layer photoresist; then, a Pd(5 nm)/ Zn(20 nm)/Pd(20 nm)/Au(700 nm) metal contact is deposited by e-beam evaporation. The widths of the grid and bus bar are 20 µm and 150 µm, respectively, and the spacing between the grid fingers is 300 µm. The total coverage of the solar cell active area by the metallization is 4%. After the metal layer is lifted off, the highly doped 100 nm p++ GaAs contact layer is selectively removed by plasma etching. The thin-film solar cells are annealed in air for 1 h at 200 °C to form ohmic contacts. An anti-reflection coating bilayer composed of 49 nm thick TiO<sub>2</sub> and 81 nm thick MgF<sub>2</sub> is deposited by e-beam evaporation. The solar cells on the plastic sheet are covered by a plastic film to protect them from debris generated during dicing along the etched trench using a CO<sub>2</sub> laser cutter (50 W; Universal Laser Systems, Scottsdale, AZ USA) with 2.5 W power and 500 pulses per inch (see Supplementary Information SI 1 and Supplementary Movie, laser cutting, for details).

#### Vacuum-assisted thermoforming of the CPCs

Figure 1b shows the schematic illustration of the vacuum-assisted thermoforming process for CPC fabrication. The polyethylene terephthalate glycol-modified (PETG) sheet is fixed with Kapton<sup>®</sup> tape across the top of a metal mold containing holes at its base. While vacuum is applied through the holes, the assembly is placed in an oven at 60 °C. The PETG is drawn into the mold as the oven temperature is raised to 96 °C for ~15 min, forming a compound parabolic shape. The CPC is then cooled, after which the CPC is detached from the metal mold.

#### Characterization of the concentrated GaAs photovoltaic

An Oriel solar simulator (model: 91191) with a Xe arc lamp and an AM 1.5 Global filter is used for *I-V* measurements obtained with an Agilent 4155B parameter analyzer. The simulator intensity is calibrated using a National Renewable Energy Laboratory (NREL)-certified Si reference cell with a diameter of 5 mm. The light incident angle is adjusted using an optical fiber and rotation stage (Newport, Irvine, CA USA, 481-A). The concentration factor under diffuse illumination (N-BK7 ground glass diffusers, 220 grit polish, Thorlabs, Newton, NJ USA) is measured with an identical setup. The solar cell operating temperature is measured by a thermal imaging camera (A325, FLIR, Wilsonville, OR USA).

#### Cost estimations

The manufacturing costs of solar cells grown by metal organic vapor phase epitaxy (MOVPE) on 6-inch-diameter round wafers are estimated based on the consideration of 24% cell efficiency, \$150 per 6inch wafer with a 27% area loss, 50 wafer reuses for both conventional ELO and ND-ELO processing, 30% and 20% group III and V precursor utilization yields, 15  $\mu$ m h<sup>-1</sup> growth rate, 70% CMP process yield, 9% margin and miscellaneous expenditures (material costs, labor, maintenance, utilities and equipment depreciation).<sup>17</sup> Module material costs are estimated using existing crystalline Si manufacturing costs without considering the expenses for module assembly (e.g., depreciation and labor).<sup>18</sup>

#### **RESULTS AND DISCUSSION**

#### Accelerated ND-ELO and laser dicing

Figure 1a shows the fabrication sequence of the thin-film GaAs solar cells via the combination of rapid ND-ELO and cold-weld bonding. The previously described ND-ELO method employs epitaxial protective layers grown between the sacrificial layer and the wafer that completely preserve the original wafer surface quality, even at the atomic scale, during the ELO process.<sup>9,10</sup> Selective removal of the protective layers using wet chemical etching eliminates the need for the chemomechanical polishing used in conventional ELO. Therefore, ND-ELO allows for the nearly indefinite reuse of the GaAs substrates, converting their cost from a material expense into a capital investment. To accelerate the conventional ELO that takes several hours to separate the active epitaxy from even a small wafer, a 350-nm-thick Au layer deposited onto the epitaxial layer surface is photolithographically patterned to form a mask for the formation of an array of mesas separated by 500-µm-wide trenches by wet chemical etching that terminates at the active solar cell epitaxy/AlAs sacrificial layer interface (see the section on 'Materials and Methods'). The bar-shaped solar cells provide approximately 21% higher utilization of the wafer active area compared with a single, square-shaped substrate cell (Supplementary Information SI 1).

Immediately following the mesa etching, the sample is cold-weldbonded to a Cr/Au (4 nm/350 nm) coated 25  $\mu$ m thick E-type Kapton<sup>®</sup> sheet, where the patterned Au on the wafer is used for the bonding interface.<sup>9,19,20</sup> Then, the bonded sample is submerged in dilute, hot HF to lift-off etch the die in 30 min. This process takes >5 h for a 5-cm-diameter wafer using conventional ELO under similarly optimized etching conditions, corresponding to a >10× reduction in process time.<sup>9</sup> Next, the lifted-off bars are fabricated into photovoltaic cells<sup>9</sup> and then separated along the trenches using a CO<sub>2</sub> laser scriber (see 'Materials and Methods' and Supplementary Information SI 1) with a kerf of ~300 µm.

**Thermoforming of plastic-CPC and adhesive-free transfer printing** Figure 1b illustrates the thermoforming process used in fabricating the mini-CPCs. The process employs three molds: a metal mold to shape the thermoformed CPC, another for making an elastomeric stamp to transfer the solar cells onto the substrate, and a third to assist in solar cell alignment.

The process for fabricating the CPCs and integrating them with the solar cells is as follows: A 0.75 mm thick PETG sheet is employed for the concentrators due to its low glass transition temperature (81 °C), making it possible to shape by simultaneously applying heat and vacuum (see 'Materials and Methods').<sup>21</sup> To transfer the diced, thin-film solar cells onto the thermoformed CPCs, an elastomeric PDMS stamp is prepared using an acrylonitrile butadiene styrene plastic mold (Figure 1c) shaped using a 3D printer. The CPC and Kapton<sup>®</sup> sheet beneath the solar cell strip are coated with Pd/Au (5 nm/100 nm) deposited through a shadow mask using electron beam evaporation. The solar cell strips are picked up by the PDMS stamp and transferprinted onto the Au-coated plastic CPC via adhesive-free low-pressure cold-weld bonding (Figure 1c).<sup>19</sup> A pyramid-shaped fixture is used to align the solar cell to the CPC without contacting its side walls (Supplementary Information SI 2). Subsequently, the CPC is coated by a 500-nm-thick reflective Ag layer using vacuum thermal evaporation while screening the solar cell with a shadow mask. The metallic mirror coating can potentially enhance the CPC reliability under ambient and solar illumination conditions. Figure 1d shows images of the CPC and thin-film GaAs solar cells at several stages of fabrication.

## Characterization of the integrated CPC/thin-film GaAs solar cell assemblies

The CPC consists of two rotated half parabolas joined together to achieve an acceptance angle that is determined by their tilt angle.<sup>22</sup> The application of CPCs for solar energy generation has thus far primarily focused on solar thermal energy conversion.<sup>23</sup> In fact, the combination of CPCs with photovoltaic cells has, up to this point, been limited by their unwieldy form factor and high aspect ratios and production costs compared with lens or mirror-based concentrators. To overcome this shortcoming, we employed a highly truncated (>90%) design using low-cost plastic materials and fabrication processes. The combination of their high truncation ratios and half cylindrical symmetries enables concentration over a wide range of incident angles, thus completely eliminating the need for active tracking systems (Supplementary Information SI 3).

Figure 2a shows the current–voltage (*I–V*) characteristics of the thin-film GaAs solar cells measured under simulated AM 1.5 G illumination at 1 sun (100 mW cm<sup>-2</sup>) intensity, both in a conventional

planar configuration and integrated with variously shaped thermoformed CPCs with a fixed aspect ratio of 4 (corresponding to 2.5-mm-wide solar cells with 10 mm high CPCs). The dependence of the concentration factor on the tilt angles of the axes of the parabolas, as inferred from the I-V characteristics, along with the calculated values, is provided in Figure 2b. A maximum concentration factor of 3.6 is achieved using a CPC with a 2.5° axis tilt. The ND-ELO processed solar cell performance has a PCE=18.4% and 17.9% with and without a 6° tilted CPC, respectively (Supplementary Information SI 4). The improved PCE using the concentrator is due to the increased open circuit voltage at a higher light intensity.

Figure 2c shows both the measured and the calculated values of the concentration factors as functions of the solar incidence angle for the 92% height-truncated, 6° tilted CPC under both direct and diffuse illumination. The 6° tilted CPC provides full concentration within  $\pm$ 6° from normal incidence. Light collection beyond this angle is enabled by the truncation of the CPC (Supplementary Information SI 3). Therefore, there is a sudden transition of the concentration

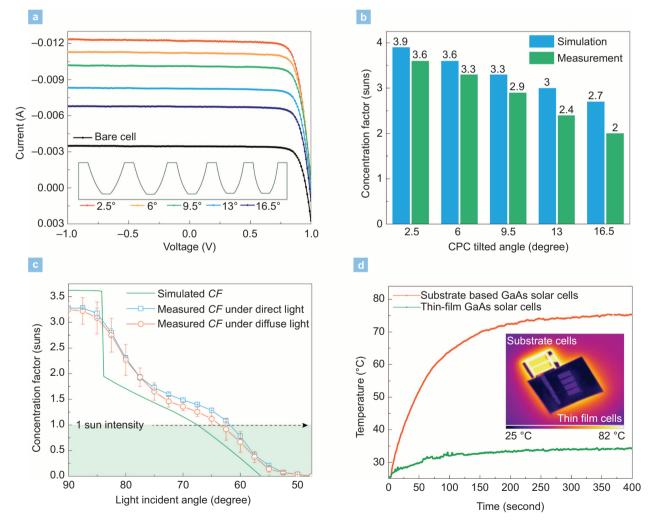


Figure 2 Performance of thin-film GaAs solar cells and plastic mini-CPCs (a) Current *versus* voltage (*I–V*) characteristics of thin-film GaAs solar cells with and without various CPCs measured under 1 sun, AM 1.5 G simulated solar illumination. Inset shows the shape of each CPC along with their corresponding tilt angles. (b) Concentration factors depending on the tilt angle of the CPCs. Blue and green bars show simulated and measured concentration factors under AM 1.5 G solar illumination, respectively. (c) Light incident angle dependent concentration factors for thin-film GaAs solar cells integrated with 6° tilted plastic mini-CPCs. The green solid line shows the simulated value. Blue and red dots with guide lines show the measured concentration factors under diffuse illumination, respectively. (d) Operating temperatures of thin-film and substrate-based GaAs solar cells under AM 1.5 G simulated solar illumination at 3.3 suns concentration, measured using an IR camera. The inset shows the cell IR camera images. CPC, compound parabolic concentrator; IR, infrared.



factor at an incidence angle of 84° in Figure 2c. The measured peak concentration factor is 3.3, corresponding to 76% of the light incident on the concentrator aperture being directed onto the cell. The actual optical element also has an approximately 10° wider acceptance angle than calculated. Concentration losses are due to the rough light-scattering surfaces that result from the imperfect shape of the metal mold and distortions created by the non-uniform thermal expansion of the PETG during thermoforming.

The light concentration as a function of the incidence angle was also characterized under diffuse illumination (see 'Materials and Methods'). As a result of the wide collector acceptance angle, the measured concentration factor has a maximum of 3.2 suns, which is nearly identical to that obtained for specular illumination at normal incidence (Figure 2c). The reduced sensitivity of the light concentration to solar position under diffuse, as well as direct sunlight confirms that the truncated CPC eliminates the need for active tracking. The thermal performance of both substrate-based and thin-film GaAs solar cells under 3.3 suns concentration is shown in Figure 2d. Infrared images taken without heat sinking at an ambient temperature of 23.6 °C are shown in the inset. The thin-film cells are mounted onto a 700 nm thick Au film that is used for the contact, rear-side mirror, cold-weld bonding material and heat sink. The cells exhibit a 17 °C lower temperature under 1 sun illumination compared with analogous cells on a 350 µm thick GaAs substrate and a 41 °C lower operating temperature under 3 suns intensity (Supplementary Information SI 5, and Supplementary Movie, thermal performance). The near room temperature operation of thin-film solar cells is advantageous because every 10 °C increase leads to a decrease in the PCE of ~0.7%.<sup>24</sup>

## Enhanced annual energy harvesting using CPC/thin-film GaAs solar cell assemblies

As noted, the mini-CPC is cylindrically symmetric, suggesting that it should be aligned along an east-west axis to provide the widest

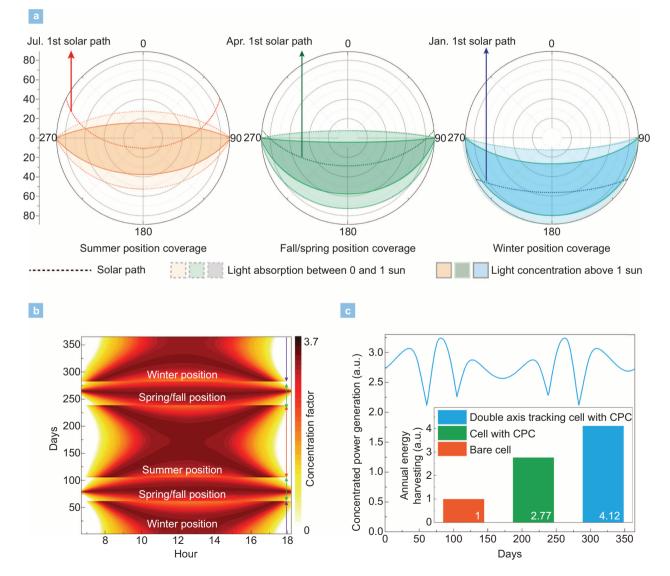


Figure 3 Optimal alignment of CPCs for maximum annual energy harvesting. (a) Polar plots showing coverage of a CPC at its optimal seasonal positions. (b) Contour plot of daily and hourly concentration factors in Phoenix, AZ, USA, using a 6° tilted CPC. (c) Ratio of the daily concentrated energy harvesting factor for thin-film GaAs solar cells with a 6° tilted CPC compared to a cell without concentration. Inset: summary of annual power generation calculated from the integration of hourly and daily energy harvesting using thin-film GaAs solar cells with and without concentrators. CPC, compound parabolic concentrator.

coverage of sunlight throughout the day simply by tilting its axis toward the zenith of the solar declination path, with only occasional seasonal adjustments to the tilt. The optimal seasonal alignments in Phoenix, AZ (33.4°N, 112.1°W), are provided in Figure 3a (Supplementary Information SI 6). We show the solar path at specific dates (1 January, 1 April and 1 July) and the coverage of the 6° tilted CPC at seasonally adjusted tilt angles (i.e., adjusted to zenith angles of 11°, 31° and 53.5° at the summer solstice, spring/fall equinoxes and the winter solstice, respectively).

Figure 3b shows the daily and hourly trends of concentrated power generation using the 6° tilted CPC. The wide CPC acceptance angle allows for energy harvesting during the most useful hours of daylight straddling midday. Figure 3c shows the result of concentrated energy harvesting throughout the year using a thin-film GaAs solar cell with a 6° tilted CPC compared to conventional, non-concentrated cells. Both cases are calculated based on three seasonal positional adjustments each year. The inset of Figure 3c compares the annual energy generation of concentrated and non-concentrated thin-film GaAs solar cells. We find that the total annual energy yield is  $2.8 \times$  higher for the concentrated cells.

#### Production cost estimation

Ultimately, the most important figure of merit for any solar cell technology is the cost of energy generation. Hence, Figure 4 shows the estimated cost reductions using the combination of approaches demonstrated here compared with conventional GaAs-based methods.<sup>17,18</sup> We assume a 24% module efficiency and  $50 \times$  wafer reuse for both

conventional ELO with wafer polishing and the ND-ELO process. This analysis indicates an approximately 97% cost reduction using the ND-ELO thin-film GaAs solar cell integrated with a 6° tilted CPC compared with substrate-based cells and an 89% reduction compared with conventional ELO-processed thin-film solar cells. Here, 66% of the reduction is due to improved epitaxial-substrate utilization using ND-ELO and 25% is from the area reduction of  $2.8 \times$  afforded by the mini-CPCs. The cost of CPC fabrication is estimated at <1% of the total module production cost (Supplementary Information SI 8). Ultimately, the costs can be dramatically reduced from \$55.97/W<sub>p</sub> for the current substrate-based single junction GaAs solar cells to only \$0.34/Wp by employing ND-ELO processed cells integrated with mini-CPCs, representing a potential cost reduction of 99.4% (Supplementary Information SI 8). The production cost estimate for the thin-film GaAs solar cell/CPC assemblies satisfies the target of \$0.5/ W<sub>p</sub> set by the US Department of Energy and is competitive with the current manufacturing cost of crystalline Si solar cell modules (\$1.19/ W<sub>p</sub>-\$0.79/W<sub>p</sub>).<sup>18</sup> Furthermore, the lightweight module impacts the balance of the system cost by minimizing the expenses incurred upon installation and racking, thus making it adaptable to rooftop installations that may not be capable of supporting heavy, unwieldy modules and bulky, active solar tracking concentrator systems.

#### CONCLUSIONS

In summary, we demonstrated thin-film GaAs solar cells integrated with low-cost, thermoformed, lightweight and wide acceptance angle

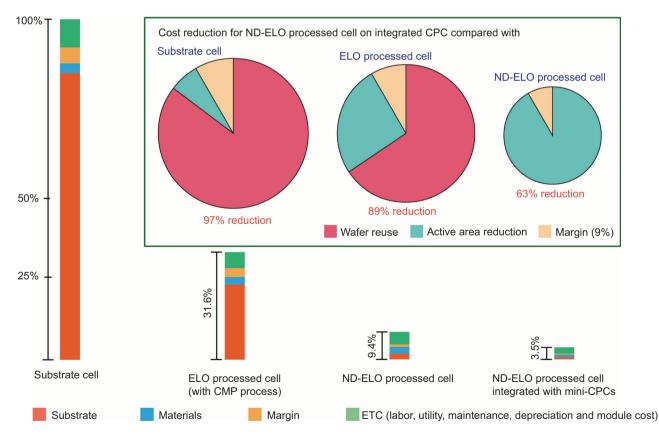


Figure 4 Comparison of production cost using thin-film GaAs solar cells integrated with CPCs. Comparison of solar cell production cost for the substrate-based, ELOprocessed and ND-ELO-processed thin-film GaAs solar cell modules with and without the 6° tilted CPC. The percentages show the relative costs compared to a conventional non-lifted-off (substrate) cell lacking concentration. The inset shows the cost reduction for the major steps used in the fabrication of the ND-ELO processed thin-film GaAs solar cells integrated with CPCs compared with a non-concentrated substrate-based cell and a conventional ELO-processed cell. CPC, compound parabolic concentrator; ELO, epitaxial lift-off; ND-ELO, non-destructive epitaxial lift-off.

#### doi:10.1038/lsa.2015.61

mini-CPCs. The fabrication combines rapid ND-ELO thin-film cells that are cold-welded to a foil substrate and are subsequently attached to the CPCs in an adhesive-free transfer printing process. The combination of the low-temperature operation of the thin-film solar cells with the highly truncated low-profile plastic CPCs provides  $2.8 \times$  enhanced energy harvesting throughout the year without the need for active solar tracking while eliminating losses incurred at the high operating temperatures characteristically encountered in concentration systems. Additionally, the combination of the potentially low cost fabrication and lightweight materials enables significant reductions in the balance of the system costs. This demonstration represents a significant step toward removing the cost barriers to the widespread deployment of lightweight and high performance thin-film GaAs solar cells in terrestrial and commercial solar electricity generation applications.

#### ACKNOWLEDGEMENTS

The authors thank Aaron Lamoureux for assistance in laser dicing. We also acknowledge the financial support of NanoFlex Power Corp.

- Green MA, Emery K, Hishikawa Y, Warta W, Dunlop ED. Solar cell efficiency tables (version 44). Prog Photovoltaics Res Appl 2014; 22: 701–710.
- 2 Chen X, Jia B, Zhang Y, Gu M. Exceeding the limit of plasmonic light trapping in textured screen-printed solar cells using Al nanoparticles and wrinkle-like graphene sheets. *Light Sci Appl* 2013; 2: e92, doi:10.1038/lsa.2013.48.
- 3 Guo CF, Sun T, Cao F, Liu Q, Ren Z. Metallic nanostructures for light trapping in energy-harvesting devices. *Light Sci Appl* 2014; 3: e161, doi:10.1038/lsa.2014.42.
- 4 Kosten ED, Atwater JH, Parsons J, Polman A, Atwater HA. Highly efficient GaAs solar cells by limiting light emission angle. *Light Sci Appl* 2013; 2: e45, doi:10.1038/ lsa.2013.1.
- 5 Kayes BM, Nie H, Twist R, Spruytte SG, Reinhardt F *et al.* 27.6% conversion efficiency, a new record for single-junction solar cells under 1 sun illumination. In: Proceedings of 2011 37th IEEE Photovoltaic Specialists Conference; 19–24 June; Seattle, WA, USA. IEEE: New York, USA, 2011, pp. 000004–000008.
- Miller OD, Yablonovitch E, Kurtz SR. Strong internal and external luminescence as solar cells approach the Shockley–Queisser limit. *IEEE J Photovoltaics* 2012; 2: 303–311.
  Steiner MA, Geisz JF, García I, Friedman DJ, Duda A *et al.* Optical enhancement of the
- Shockley W, Queisser HJ. Detailed balance limit of efficiency of p-n junction solar
- Shockley W, Queisser HJ. Detailed balance limit of efficiency of p-n junction solic cells. J Appl Phys 1961; 32: 510.

- 9 Lee K, Zimmerman JD, Hughes TW, Forrest SR. Non-destructive wafer recycling for low-cost thin-film flexible optoelectronics. Adv Funct Mater 2014; 24: 4284–4291.
- 10 Lee K, Zimmerman JD, Xiao X, Sun K, Forrest SR. Reuse of GaAs substrates for epitaxial lift-off by employing protection layers. *J Appl Phys* 2012; **111**: 033527.
- 11 Cheng CW, Shiu KT, Li N, Han SJ, Shi L et al. Epitaxial lift-off process for gallium arsenide substrate reuse and flexible electronics. Nat Commun 2013; 4: 1577.
- 12 Bauhuis GJ, Mulder P, Haverkamp EJ, Schermer JJ, Bongers E et al. Wafer reuse for repeated growth of III–V solar cells. Prog Photovoltaics Res Appl 2010; 18: 155–159.
- 13 Yoon J, Jo S, Chun IS, Jung I, Kim HS et al. GaAs photovoltaics and optoelectronics using releasable multilayer epitaxial assemblies. *Nature* 2010; 465: 329–333.
- 14 Kurtz SR. Opportunities and challenges for development of a mature concentrating photovoltaic power industry. NREL: Washington, DC, USA, 2012. NREL/TP-5200-43208.
- 15 Memarian M, Eleftheriades GV. Light concentration using hetero-junctions of anisotropic low permittivity metamaterials. *Light Sci Appl* 2013; 2: e114, doi:10.1038/lsa.2013.70.
- 16 Rabl A. Comparison of solar concentrators. Sol Energy 1976; 18: 93-111.
- 17 Woodhouse M, Goodrich A. A manufacturing cost analysis relevant to single and dual junction photovoltaic cells fabricated with III–Vs and III–Vs grown on Czochralski Silicon. NREL: Washington, DC, USA, 2014. NREL Rep. No. PR-6A20-60126 92.
- 18 Goodrich A, Hacke P, Wang Q, Sopori B, Margolis R et al. A wafer-based monocrystalline silicon photovoltaics road map: utilizing known technology improvement opportunities for further reductions in manufacturing costs. Sol Energy Mater Sol Cells 2013; 114: 110–135.
- Ferguson GS, Chaudhury MK, Sigal GB, Whitesides GM. Contact adhesion of thin gold films on elastomeric supports: cold welding under ambient conditions. *Science* 1991; 253: 776–778.
- 20 Lee K, Shiu KT, Zimmerman JD, Renshaw CK, Forrest SR. Multiple growths of epitaxial lift-off solar cells from a single InP substrate. *Appl Phys Lett* 2010; 97: 101107.
- 21 Xu X, Davanco M, Qi X, Forrest SR. Direct transfer patterning on three dimensionally deformed surfaces at micrometer resolutions and its application to hemispherical focal plane detector arrays. *Org Electron* 2008; **9**: 1122–1127.
- 22 Rabl A. Optical and thermal properties of compound parabolic concentrators. Sol Energy 1976; 18: 497–511.
- 23 Kalogirou SA. Solar thermal collectors and applications. Prog Energy Combust Sci 2004; 30: 231–295.
- 24 Fan JCC. Theoretical temperature dependence of solar cell parameters. *Sol Cells* 1986; **17**: 309–315.

This work is licensed under a Creative Commons Attribution-

NonCommercial-NoDerivs 3.0 Unported License. The images or other third party material in this article are included in the article's Creative Commons license, unless indicated otherwise in the credit line; if the material is not included under the Creative Commons license, users will need to obtain permission from the license holder to reproduce the material. To view a copy of this license, visit http://creativecommons.org/licenses/ by-nc-nd/3.0/

Supplementary information for this article can be found on the Light: Science & Applications' website (http://www.nature.com/lsa/).